From bulk materials to nanoparticles using a one-step electrochemical method

2008 J. Phys.: Condens. Matter 20 204104

(http://iopscience.iop.org/0953-8984/20/20/204104)

J. Phys.: Condens. Matter **20** (2008) 204104 (5pp) doi:10.1088/0953-8984/20/20/204104

From bulk materials to nanoparticles using a one-step electrochemical method

S Neveu[1], **R Massart, V Rocher and V Cabuil**

Labo LI2C, University Pierre et Marie Curie (Paris 6), CNRS UMR 7612, 4 place Jussieu, Paris, F-75232, France

E-mail: sophie.neveu@upmc.fr

Received 1 April 2008
Published 1 May 2008
Online at stacks.iop.org/JPhysCM/20/204104

Abstract

This paper describes an electrochemical method which permits us to transform solid metals (cobalt, iron or nickel) into nanoparticles. An electrolysis cell is made, the anode being a metal bar and the cathode a mercury layer. Magnetic nanoparticles are obtained in one step by electroreduction of mercury. Electrolysis is performed in an aqueous medium at pH above 6 in order to avoid the reduction of protons. The magnetic nanoparticles obtained are kept in mercury and can be recovered in an organic solvent.

1. Introduction

The first mercury based magnetic fluid was prepared by Luborsky [1]. It was made of iron nanoparticles dispersed in mercury. Later, two groups described the synthesis of iron, cobalt, nickel or alloy particles in mercury [2–7]. In these works, cathodic reduction was performed in an acidic medium; as redox potential E_{H^+/H_2} is higher than redox potential $E_{M^{2+}/M}$, protons oxidized the metal. In a recent work [8], this problem has been overcome for cobalt in mercury by performing the electrolytic reduction at a pH for which the cobalt is not oxidized by the protons. However, in all these studies, the anode was a Pt one and the amount of metal particles incorporated in mercury was limited by the amount of metallic ions in solution.

In this study, a simple and original method for synthesizing nanoparticles in mercury is proposed. It consists in the transformation of bulk metal into nanoparticles in an electrochemical way in aqueous solution. The anode is a metal bar (Fe, Co or Ni) which is oxidized into metal ions (Fe^{2+}, Co^{2+} or Ni^{2+}). The electrolytic solution is an aqueous solution of the same ions. The metal species are then reduced on the mercury cathode producing metal nanoparticles that are directly dispersed in mercury. The system thus obtained is a magnetic and conducting fluid that can be considered as a source of metal nanoparticles which can be recovered by using liquid–liquid extraction.

[1] Present address: Labo LI2C, University Pierre et Marie Curie (Paris 6), CNRS UMR 7612, 4 place Jussieu, Paris, F-75232, France.

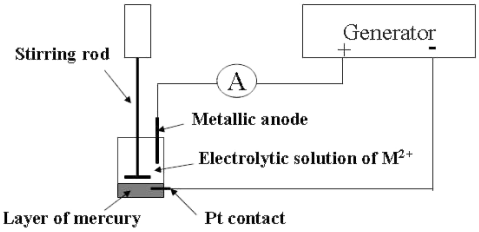

Figure 1. Experimental set-up of the electrolysis device.

2. Experimental details

2.1. Electrolytic transfer of metal from the anode to the mercury

Electrolysis experiments were performed using a generator (Delta Electronika, Power Supply E030-1) under constant stirring, for at least 3 h at room temperature. The cathode was a platinum rod in contact with the mercury. The anode was a metal rod (Fe, Co or Ni, provided by Goodfellow with a purity of 99%). The set-up of the experiment is shown in figure 1.

The electrolysis was performed in aqueous solutions of metal cations and either a mixture of trisodium citrate (0.7 mol l^{-1}), with citric acid (0.28 mol l^{-1}), and sodium chloride (0.1 mol l^{-1}) at pH 6.5 (a solution denoted as [Cit]) or a mixture of sodium citrate (0.6 mol l^{-1}), sodium chloride (0.1 mol l^{-1}) and ammonia (0.66 mol l^{-1}) at pH 9.5 (a solution denoted as [Cit + NH_3]). When Fe^{2+} was used, it was necessary to work under nitrogen atmosphere in order to avoid oxidation in Fe^{3+}.

Table 1. Electrolysis results: Δn_a, amount of metal oxidized at the anode; q, amount of electricity in Faraday's constant (96500 C.mol^{-1}); Δn_s, amount of metal ions in solution; m_{Hg}, mass of mercury; ϕ, volume fraction of iron in mercury.

Sample	Medium	$\Delta n_a \times 10^2$ (mol)	$q \times 10^2$	$\Delta n_s \times 10^3$ (mol)	$\Delta n_s/\Delta n_a \times 10^2$	m_{Hg} (g)	$\Phi \times 10^3$
Co37	[Cit]	2.38	4.47	1	5	353	6.03
Co21	[Cit + NH_3]	2.2	4.47	−3.3	−5	338	5.82
Fe25	[Cit]	2.3	4.58	−1.36	−2.7	331	6.57
Fe39	[Cit]	2.29	4.52	0	0	323	6.58
Ni22	[Cit + NH_3]	1.08	2.38	−0.56	−5	325	2.97
Ni16	[Cit]	1.40	2.83	14.8	100	334	
Ni19	[NH_3]	1.6	3.83	2	12	343	4.05

The metal species were $(Fe(NH_4)_2(SO_4)_2{\cdot}6H_2O$, $CoCl_2{\cdot}6H_2O$ or $NiCl_2{\cdot}6H_2O)$. Their initial concentrations were of the order of 0.2 mol l^{-1}. The amount of initial cations is denoted as n_s (mole number). The amount of metal oxidized at the anode, denoted as Δn_a, was determined by the decrease of the weight of the anode during the electrolysis.

During the electrolysis, the intensity I and difference of potential ΔV were constant. The intensity I was equal to 0.4 A (the current density was equal to 26 A m^{-2}). The mercury weight was approximately 300 g. The amount of variation of metal ions in solution, denoted as Δn_s, was determined by atomic absorption spectrophotometry using a Perkin-Elmer AA100 Analyst.

2.2. Magnetization characterizations

Magnetic measurements were carried out on mercury magnetic fluid using a Foner device [9]. The magnetic fluid was sampled in a 1 ml bottle settled at the top of a vibrating stalk located in an electromagnet. The field varied from 0 to 1 T (10 000 Oe).

2.3. Extraction of the metal nanoparticles from the mercury

Magnetic particles dispersed in mercury can be extracted from it, using a mixture of surfactant in an organic solvent. 10 g of magnetic mercury (with a magnetic material volume fraction equal to 0.015) and 10 ml of solvent (surfactant in cyclohexane) were mixed by mechanical stirring for four days. The surfactant used was trioctylphosphineoxide (TOPO), a well-known stabilizer of metal particles [10]. A black magnetic precipitate was obtained in the organic solution. This precipitate was washed several times with acetone and alcohol and then dried.

2.4. X-ray diffraction

The x-ray diffraction measurements were performed using a STOE Stadi P goniometer with a Siemens Kristalloflex x-ray generator with a cobalt anticathode ($\lambda = 1.7809$ Å) driven by a personal computer through a DACO–MP interface. These measurements were done on the magnetic particles after drying in air.

2.5. Transmission electron microscopy (TEM)

The transmission electron microscopy was performed with a Jeol JEM100CX2 microscope, on the magnetic particles obtained after extraction. An organic dispersion of particles is dropped on a copper grid covered by an amorphous carbon shell.

3. Results

3.1. Electrolysis results

The results of the electrolysis are summarized in table 1.

The amount of moles of metal oxidized at the anode, Δn_a, is, as expected, half of the amount of electricity q in farads ($q = i(t)t(s)/96\,500$ C) assuming that the anodic reaction is $M \rightarrow M^{2+} + 2e^-$

Atomic absorption spectroscopy showed that the metal ion concentration in solution remained almost constant during the electrolysis ($\Delta n_s/\Delta n_a < 5 \times 10^{-2}$). Therefore, all the M^{2+} produced by the anodic reaction is reduced in metallic iron at the mercury cathode: $M^{2+} + 2e^- \rightarrow M_{Hg}$ and the total reaction in the electrolytic device is a transfer of iron from the anode to the mercury cathode: $M_{Anode} \rightarrow M_{Hg}$.

The volume fraction of iron in mercury is calculated from $\phi = \frac{V_M}{V_{Hg}+V_M} = \frac{\Delta n_a V_{m(M)}}{\frac{m_{Hg}}{\rho_{Hg}}+\Delta n_a V_{m(M)}}$ where $V_m(M)$ is the molar volume in m^3 mol^{-1} (6.62×10^{-6} for Co, 7×10^{-6} for Fe, 6.60×10^{-6} for Ni), m_{Hg} and ρ_{Hg} (13.6 g cm^{-3}) are the mass and the density of mercury. In the case of the sample Ni16 (nickel in citrate medium), the total amount of Ni^{2+} produced at the anode remained in solution ($\Delta n_s/\Delta n_a = 1$) and was not reduced at the cathode. Moreover, a dihydrogen release was observed at the cathode.

3.2. Characterization of the mercury based magnetic fluid

Magnetization measurements were performed in the case of cobalt and iron, but nickel sample magnetizations were too low to provide a sufficient signal using a Foner device. The curve $M = f(B)$ obtained by increasing the field followed Langevin's law [11]: $M = M_s[\coth(\frac{\mu B}{kT}) - (\frac{kT}{\mu B})]$ where M_s is the saturation magnetization of the solution. T is the absolute temperature, k the Boltzmann constant and B the magnetic induction; μ is the magnetic moment of the particles.

Magnetization curves obtained for samples Co37 and Fe25 are shown in figures 2 and 3. The effective saturation magnetization of the magnetic material m_s can be deduced from $m_s = M_s/\phi$ where ϕ is the volume fraction of particles deduced from the experimental electrochemical results.

For Co37, $m_s(Co) = 1070$ kA m^{-1} and for Fe25, $m_s(Fe) = 1000$ kA m^{-1}. These values are lower than those

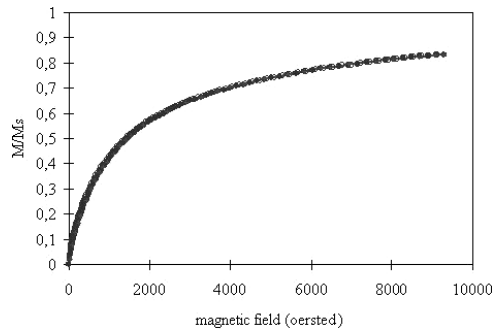

Figure 2. Magnetization curve of iron nanoparticles in mercury: sample Fe25, $d_0 = 5.6$ nm, $\sigma = 0.01$.

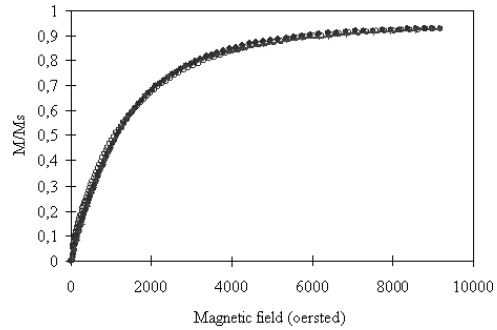

Figure 3. Magnetization curve of cobalt nanoparticles in mercury: sample Co37, $d_0 = 4.8$ nm, $\sigma = 0.08$.

for the corresponding bulk materials (1400 kA m^{-1} for cobalt and 1700 A m^{-1} for iron). This decrease could be due to the presence of poorly crystallized particles or to the surface disorder effects [12].

Assuming that the particle size distribution can be described by a log-normal law: $P(D) = \frac{1}{D\sigma\sqrt{2\pi}} \exp(\frac{-\ln^2(\frac{D}{D_0})}{2\sigma^2})$, and that interparticle interactions are low enough that the Langevin law is followed [13], analysis of the shape of the curve allows us to determine the parameters of the particle

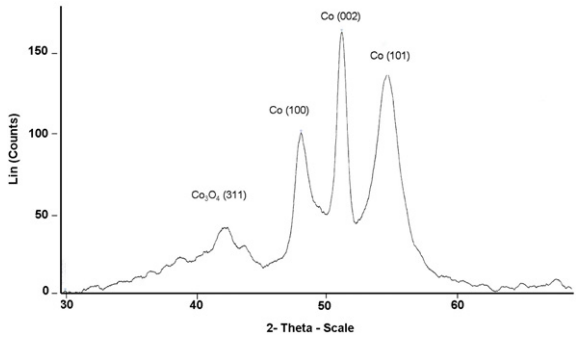

Figure 5. X-ray diffraction patterns for cobalt nanoparticles.

size distribution (D_0 and σ) [14] using the m_s value found experimentally. The mean diameter D_0 ranges between 4.7 and 6 nm and the standard deviation σ is of the order of 0.3.

3.3. Characterization of the particles obtained after extraction

Particles dispersed in mercury cannot be directly observed. In contrast, once the extraction is realized, the extracted nanoparticles have been observed by transmission electron microscopy. Figure 4 represents pictures of the particles obtained after extraction. Particles are polydispersed with a mean diameter of the order of 13 nm for cobalt (figure 4(a)) or iron particles (figure 4(b)) and 4.5 nm for nickel nanoparticles (figure 4(c)).

X-ray diffraction patterns obtained for precipitates extracted from mercury are given in figures 5, 6 and 7. The crystallographic structures of particles are compared with JCPDS data.

For cobalt particles (figure 5), the characteristic peaks of hexagonal close packed cobalt, hcp Co ((100), (002), (101)), are observed. The peak (311) is attributed to cobalt oxide Co_3O_4. For iron nanoparticles (figure 6), the crystallographic peaks are characteristic of the cubic centered structure ((110), and (200)). The peak (311) is attributed to magnetite Fe_3O_4. For nickel particles (figure 7), the characteristic peaks

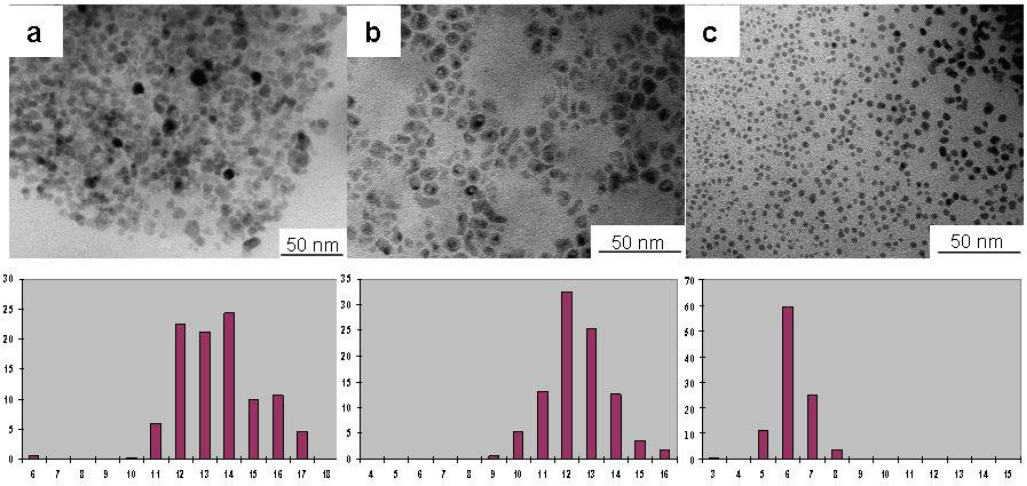

Figure 4. MET picture and the corresponding histograms of (a) cobalt nanoparticles, (b) iron nanoparticles and (c) nickel nanoparticles. The bar is 50 nm.

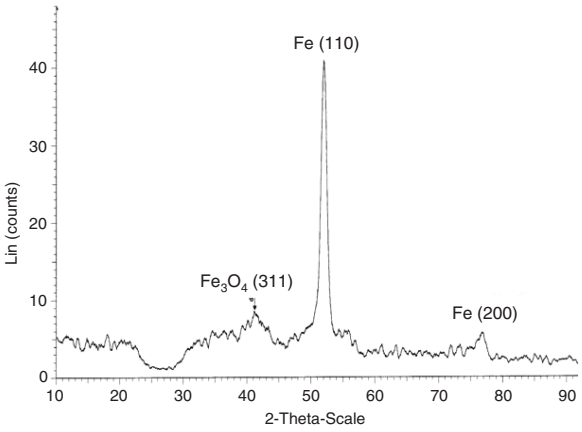

Figure 6. X-ray diffraction patterns for iron nanoparticles.

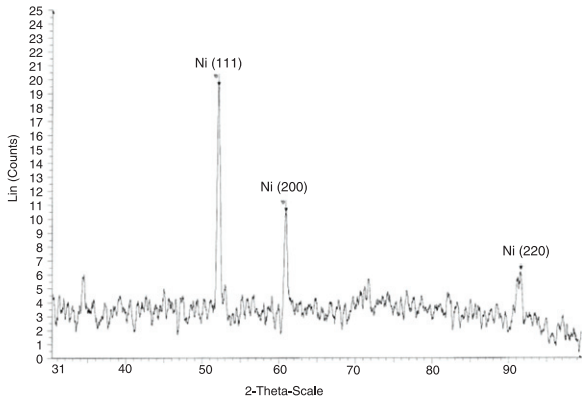

Figure 7. X-ray diffraction patterns for nickel nanoparticles.

of hexagonal close packed nickel, hcp Ni ((111), (200), (220)), are present without any additional peaks. When the nanoparticles are recovered by extraction, it seems that the cobalt and the iron nanoparticles are covered by an oxide shell. This shell seems to protect them against oxidation as the metallic structure is retained even after exposure to the air. This oxidation shell may explain the difference observed between the particles sizes obtained by transmission electron microscopy (extracted magnetic particles) and from the magnetization curve (magnetic nanoparticles in mercury).

4. Discussion

This work described an electrochemical method which consists in conversion of massive metal (Fe, Co, Ni) into metal nanoparticles dispersed in mercury by using an anodic oxidation of the metal coupled with a reduction of metal ions on a mercury cathode.

When the cathodic reduction is performed in an acidic medium, metals are oxidized by protons because the redox potential E_{H^+/H_2} (0 V at pH 0 for example) is higher than the redox potentials $E_{Fe^{2+}/Fe}$ (−0.44 V), $E_{Co^{2+}/Co}$ (−0.28 V) and $E_{Ni^{2+}/Ni}$ (−0.257 V). The choice of an electrolytic solution such as [Cit] or [Cit + NH_3] to realize the electrolytic transfer of the metal from the anode to the mercury is based on electrochemical considerations: below pH 5, Co^{2+}, Fe^{2+} or Ni^{2+} are not reducible on a mercury cathode. Table 2 allows us to compare the overvoltage values, for mercury, for Co^{2+}, Fe^{2+} and Ni^{2+} at two pH values above 5 (electrokinetic properties) [15]. In these two media, metal cations are reduced before protons.

The fact that nanoparticles can be obtained might be explained as follows: cobalt, iron and nickel are not soluble in mercury and do not allow forming an alloy with it [16, 17]. Indeed metal atoms produced by cathodic reduction coalesce and metal aggregates are formed on the cathode. At the mercury–metal interface (Hg–M interface), an interfacial potential occurs due to the difference between the work function of mercury and that of the metal (Fe, Co or Ni). The electron work functions of Fe (4.7 eV), Co (5 eV) and Ni (5.15 eV) are higher than that of the mercury (4.5 eV) [18].

Table 2. Overvoltage values, for mercury.

Media	pH	Metal cation	Overvoltage (versus SCE) (V)
Ammonium citrate/ammonia	8.5	Co^{2+}	−1.7
		Fe^{2+}	−1.7
		Ni^{2+}	−1.37
		H^+	−1.8
Ammonium tartrate/ammonia	9.5	Co^{2+}	−1.23
		Fe^{2+}	−1.41
		Ni^{2+}	−0.96
		H^+	−1.84

This means that negatively charged metal aggregates are in positively charged mercury cavities. This can explain why the nanoparticles do not aggregate and are well dispersed in mercury.

5. Conclusion

The conversion of bulk metal (Fe, Co, Ni) into metal nanoparticles dispersed in mercury is possible by an electrochemical method involving an anodic oxidation of the metal coupled with a reduction of metal ions on a mercury cathode.

Metal nanoparticles can be stored in mercury and recovered in organic solvent using a surfactant. In the case of iron or cobalt, the recovered nanoparticles are passivated by a shell of Fe_3O_4 and Co_3O_4. The diameter of the nanoparticles obtained after the extraction is around 13 nm.

The electrochemical process described in this work can be extended to other materials which do not form any alloy with mercury such as copper, chromium and platinum [17, 18]. The particle size control has also to be improved.

Acknowledgments

The authors are grateful to Aude Michel for the transmission electron microscopy pictures and Delphine Talbot for technical assistance.

References

[1] Luborsky F E and Lawrence P E 1961 *J. Appl. Phys.* **32** 231S
[2] Windle P L, Popplewell J and Charles S W 1975 *IEEE Trans. Magn.* **11** 1367
[3] Charles S W and Popplewell J 1976 *IEEE Trans. Magn.* **12** 795
[4] Charles S W and Issari B 1986 *J. Magn. Magn. Mater.* **54–57** 743
[5] Veprik I Yu and Fedonenko A I 1989 *Magnetohydrodynamics* **24** 365
[6] Alekseev V A and Fedonenko A I 1989 *Magnetohydrodynamics* **25** 57
[7] Alekseev V A, Minukov S G and Fedonenko A I 1990 *Magnetohydrodynamics* **26** 45
[8] Massart R, Rasolonjatovo B, Neveu S and Cabuil V 2007 *J. Magn. Magn. Mater.* **308** 10
[9] Foner S and Macniff E J Jr 1968 *Rev. Sci. Instrum.* **39** 171
[10] Cheon J, Kang N J, Lee S M, Lee J H, Yoon J H and Oh S J 2004 *J. Am. Chem. Soc.* **126** 1950
[11] Chantrell R W, Popplewell J and Charles S W 1978 *IEEE Trans. Magn.* **14** 975
[12] Kodama R H 1999 *J. Magn. Magn. Mater.* **200** 359
[13] Kayser R and Miskolczy G 1970 *J. Appl. Phys.* **41** 1064
[14] Bacri J C, Perzynski R, Salin D, Cabuil V and Massart R 1986 *J. Magn. Magn. Mater.* **62** 36
[15] Meites L 1965 *Polarographic Techniques* (New York: Interscience)
[16] Moffatt W G 1976 *Handbook of Binary Phase Diagrams* (New York: Genium)
[17] Massalski T B 1986 *Binary Alloy Phase Diagrams* (Metals Park, OH: American Soc. for Metals)
[18] *Handbook of Chemistry and Physics* 1984/1985 65th edn (Boca Raton, FL: CRC Press) p E76